Effectiveness of 32-element Surface Coil Array for Accelerated Volume-Targeted Breath-Hold Coronary MRA

Hyun Yeol Lee[1,2], Jin-Suck Suh[1,2], Jaeseok Park[2,3]

Purpose : To compare 12 and 32-element surface coil arrays for highly accelerated coronary magnetic resonance angiography (MRA) using parallel imaging.

Materials and Methods : Steady state free precession coronary MRA was performed in 5 healthy volunteers at 1.5 T whole body MR scanner using both 12 and 32-element surface coil arrays. Left anterior descending and right coronary artery data sets were acquired for each volunteer. Data sets were sub-sampled for parallel imaging using reduction factors from 1 to 6. Mean geometry factor (g-factor), maximum g-factor, and artifact level were calculated for each of the two coil arrays.

Results : Over all reduction factors, the mean and maximum g-factors and artifact level were significantly reduced using the 32-element array compared to the 12-element array ($P << 0.1$). The mean g-factor was sensitive to the imaging orientations of coronary arteries while the maximum g-factor and artifact level were independent of orientation.

Conclusion : The 32-element surface coil array significantly improves artifact and noise suppression for highly accelerated coronary MRA using parallel imaging. The increased acceleration factors made feasible with the 32-element array offer the potential to enhance spatial resolution or increase volumetric coverage for 3D coronary MRA.

Index words : Magnetic resonance imaging (MRI)
Coronary magnetic resonance angiography
Parallel imaging
Geometry factor

Introduction

In coronary magnetic resonance angiography (MRA), imaging data is typically acquired with a short mid-diastolic acquisition window to avoid cardiac motion artifacts. The relatively short duration of data acquisition window results in decreased imaging

JKSMRM 13:137-145(2009)
[1]Department of Medical Science, Yonsei University
[2]Department of Radiology, Yonsei University College of Medicine
[3]Department of Computational Science and Engineering, Yonsei University
Received; December 5, 2009, revised; December 23, 2009, accepted; December 24, 2009
Corresponding author : Jaeseok Park, Ph.D., Department of Radiology, Yonsei University College of Medicine,
250 Seongsanro, Seodaemun-gu, Seoul 120-752, Korea
Tel. 82-2-2228-2397 Fax. 82-2-393-3035 E-mail: jaeseokpark@yonsei.ac.kr

efficiency and thereby, prolonging the imaging time necessary to achieve sufficient spatial resolution which is required to depict vessels with small diameters.

Parallel magnetic resonance imaging (MRI) techniques (1, 2) offer the potential to overcome the limitations in coronary MRA, using arrays of multiple receiver coils. For parallel MRI, coil k-space is under-sampled in the phase encoding (PE) direction as compared to conventional data acquisition. Knowledge of spatial coil sensitivity profiles is exploited to reconstruct images from the under-sampled data. However, the acceleration is limited by the loss of signal-to-noise ratio (SNR) due to decreased imaging time as well as spatial noise amplification dependent upon coil geometry and k-space sampling pattern. In coronary imaging, SNR loss is critical due to higher resolution requirements.

The loss of SNR can be mitigated by combining parallel MRI with high-SNR pulse sequences (3) or by employing a high-field-strength system (4). SNR can also be improved by optimizing the geometry of receiver coil array (5) or k-space sampling trajectories (6, 7). Noise amplification can be reduced in image reconstruction by incorporating regularization into inversion process though spatial resolution is traded off with noise (8). However, in practice, achievable acceleration remains limited by the number of coil elements in receiver surface arrays (1). Recently, a 32-element array with smaller coil dimensions was introduced to investigate the feasibility of highly accelerated volumetric imaging (9). However, no comparison has been made between the commercial 12-element coil array and the 32-element coil array for coronary artery imaging orientations.

The purpose of this work was to compare 12 and 32-element surface coil arrays for highly accelerated coronary MRA. Experimental studies were performed in five healthy volunteers in left anterior descending (LAD) and right coronary artery (RCA) imaging orientations. The performance of coil arrays was compared using measurements of coil geometry factor (g-factor) and artifact level. This work also provides guidelines for accelerated coronary MRA with 12 and 32-element coil arrays.

Materials and Methods

Data acquisition was performed in five healthy volunteers on a 1.5 T whole body MR scanner (MAGNETOM AVANTO, Siemens Medical Solutions, Erlangen, Germany) equipped with a high performance gradient sub-system (maximum amplitude: 40 mT/m, maximum slew rate: 200 mT/m/ms). An informed written consent was obtained from each volunteer before the study, and was approved by our Institutional Review Board. During each scan, the volunteers were instructed to hold their breaths at the end of inspiration.

An electrocardiogram triggered three-dimensional (3D) segmented steady state free precession (SSFP) sequence was used to acquire both LAD and RCA data sets from each volunteer using 12 and 32-element surface coil arrays respectively. The 32-element rectangular coil array was placed anterior (16 elements, dimension of coil element: 9×10 cm^2) and posterior (16 elements, dimension of coil element: 9×10 cm^2) to each subject (Fig. 1a). Both the anterior and posterior coil arrays were composed of four elements along the body axis and four elements along the left-right direction. The 12-element rectangular surface coil array

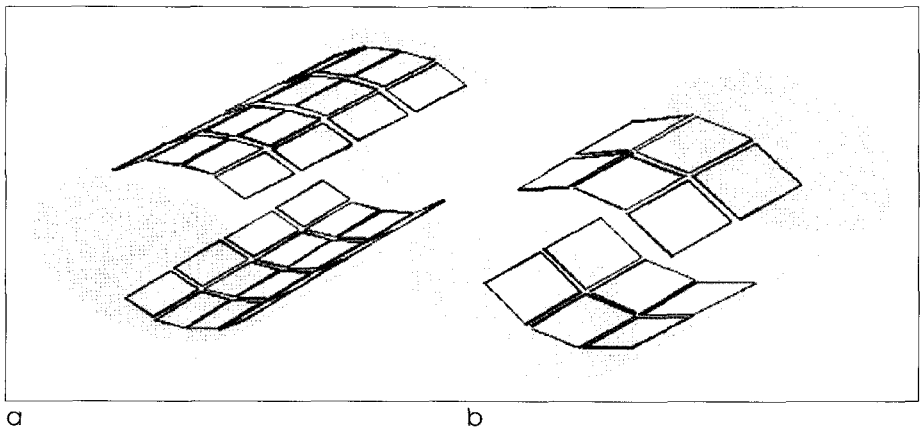

Fig. 1. Geometry of surface coil array anterior and posterior to a subject: (a) 32-element array and (b) 12-element array

was similarly placed anterior (6 elements, dimension of coil element: 11×11 cm^2) and posterior (6 elements, dimension of coil element: 11×11 cm^2) to each subject (Fig. 1b). For the later set-up, both the anterior and posterior coil arrays were composed of two elements along the body axis and three elements along the left-right direction.

The imaging parameters were as follows: TR (time of repetition) / TE (time of echo) / flip angle = 3.6 ms/1.8 ms/60°, FOV (field-of-view) = $240\text{-}260 \times 350\text{-}380$ mm^2, number of heartbeats / partition = 6, number of acquired lines / heartbeats = 35, matrix size = 210×448, breath-hold duration = 30-40 sec, slice thickness = 3 mm (interpolated to 1.5 mm), and number of partitions = 6 (interpolated to 12). A hamming windowed sinc radio-frequency (RF) pulse with 600μ sec duration was used for slab excitation. A spectral-selective fat saturation RF pulse followed by eight dummy pulses with sinusoidally varying flip angles (10) was applied to establish smooth transition of signal to steady state before data acquisition at each heartbeat. The fully acquired data was decimated by reduction factor (R) to simulate the accelerated acquisition for sensitivity encoded (SENSE) reconstruction.

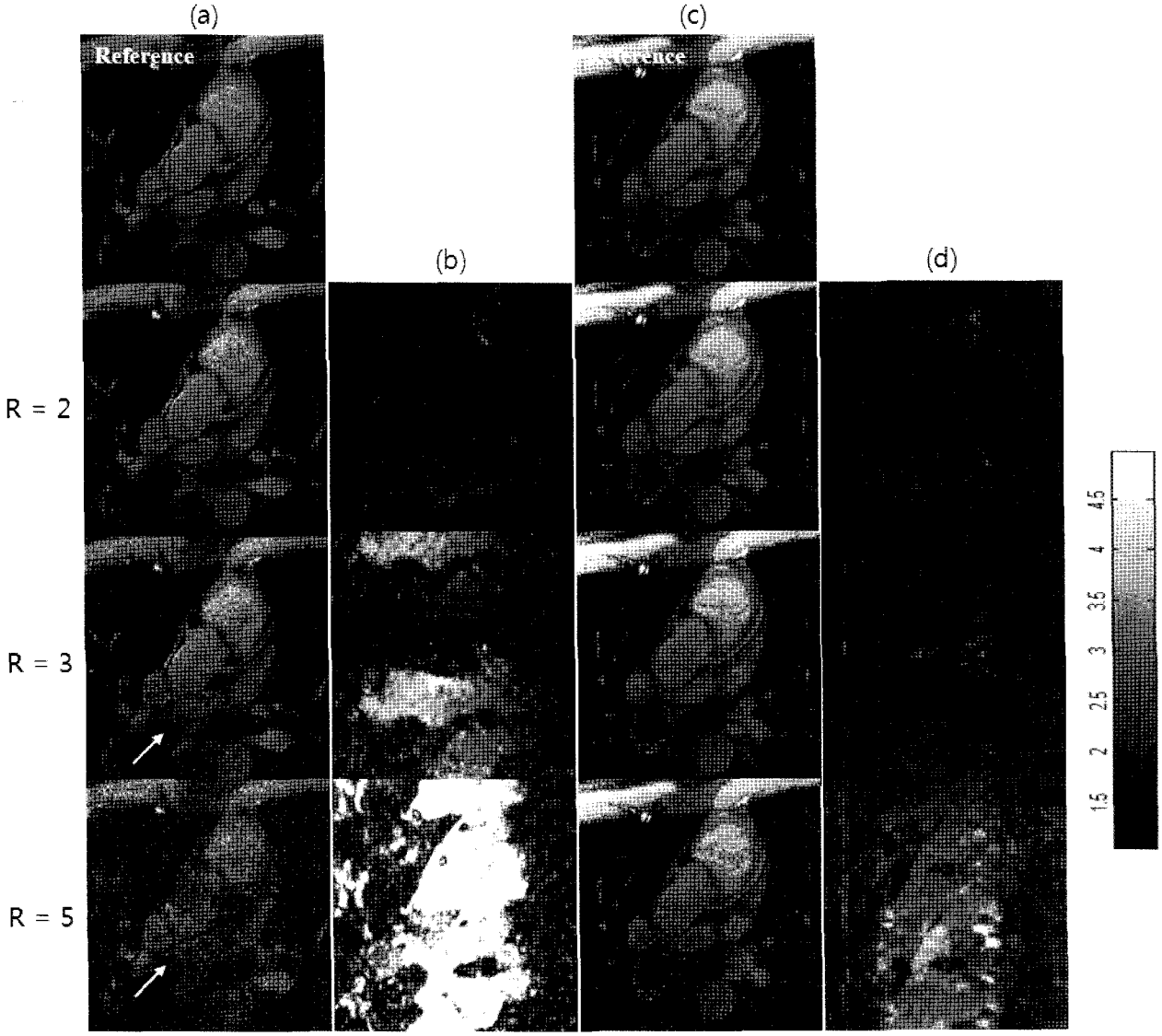

Fig. 2. SENSE images and g-factor maps reconstructed with increasing reduction factor (R): (a) SENSE images for 12-element array, (b) g-factor maps for 12-element array, (c) SENSE images for 32-element array, and (d) g-factor maps for 32-element array. Note reduced g-factor and noise with the 32-element array (c, d) over the 12-element array (a, b)

SENSE Reconstruction and g-factor Calculation

The aliased images from all the coil elements in SENSE reconstruction were formulated in the following linear system (1,8):

$$x = (S^H \psi^{-1} S)^{-1} S^H \psi^{-1} y \quad [1]$$

where x is the reconstructed image, S is the sensitivity encoding matrix, S^H is the transposed complex conjugate of the sensitivity encoding matrix, ψ is the noise covariance matrix, and y is the aliased image from all the coils. In this work, the noise covariance matrix was constructed using the pre-scanned noise data. To obtain coil sensitivity information, the central 1/4 region of k-space was extracted from the fully acquired data, zero padded, hamming windowed, and then Fourier transformed (8).

Spatial noise amplification in SENSE is quantified by coil geometry factor g:

$$g_\rho = \sqrt{\left(S^H \psi^{-1} S\right)^{-1}_{(\rho,\rho)} \left(S^H \psi^{-1} S\right)_{(\rho,\rho)}} \quad [2]$$

where the subscript (ρ, ρ) denotes the voxels to be unfolded in the full-FOV image. The g-factor depends strongly on position, and yields a high value when the SENSE inversion in Eq. [1] is ill conditioned. The ill conditioned inversion depends on the acceleration rate, the number of coils, coil sensitivity profiles, and slice geometry.

Image reconstruction and g-factor calculation were performed using the Matlab software package (MathWorks, Natick, MA).

In Vivo Studies

To compare the performance of the 12 and 32-element surface coil arrays for accelerated imaging, a fully acquired LAD data from each surface coil array was decimated by R = 2, 3, and 5. A reference image was reconstructed by SENSE using the fully acquired data. The reduced data was used for SENSE reconstruction and g-factor calculation. The g-factor map corresponding to each reduction factor was calculated and then scaled from one to five.

Noise amplification in SENSE reconstruction with the two coil arrays was investigated for the LAD data. As reduction factor increases from one to six, mean and maximum g-factors were calculated over a region-of-interest (ROI). The mean and maximum g-factors were plotted as a function of reduction factor. Additionally, artifact power (AP) was calculated from the reconstructed images with reduction factors by the following equation:

$$Artifact\ Power\ (AP) = \frac{\sum_j \left\| I_j^{REFERENCE} \right| - \left| I_j^{SENSE} \right\|^2}{\sum_j \left| I_j^{REFERENCE} \right|^2} \quad [3]$$

where j is the pixel index, $I^{REFERENCE}$ is the reference image, and I^{SENSE} is the SENSE image.

The mean g-factor, maximum g-factor, and AP for the LAD and RCA orientations respectively were compared between images produced from the five volunteers using the 12 and 32-element surface coil arrays. The sensitivity of the g-factor and AP to the two different coronary artery orientations was also estimated. A two-factor analysis of variance with replications was used to evaluate statistical difference with P-value of 0.05.

For visual comparison of the images from the 12 and 32-element surface coil arrays, both the LAD and RCA images were demonstrated after SENSE (R = 4) reconstruction and 3D maximum-intensity-projection (MIP).

Table 1. Mean g-factor, Maximum g-factor, and Artifact Power in SENSE with Five Sets of LAD Data

		R = 2	R = 3	R = 4	R = 5	R = 6	Significance
Mean g-factor	12-element	1.08±0.035	1.27±0.11	1.67±0.19	2.32±0.27	3.11±0.29	P=2.16E-09
	32-element	1.05±0.022	1.12±0.041	1.25±0.072	1.45±0.12	1.69±0.19	
Maximum g-factor	12-element	2.46±0.61	3.44±0.94	6.45±1.58	15.78±3.25	19.2±1.39	P=3.31E-08
	32-element	2.19±0.73	2.69±1.04	3.36±1.34	4.90±1.48	7.24±1.66	
Artifact Power	12-element	0.015±0.0048	0.039±0.010	0.086±0.029	0.17±0.043	0.25±0.055	P=3.58E-10
	32-element	0.012±0.0077	0.026±0.016	0.043±0.025	0.068±0.032	0.099±0.040	

Results

Figure 2 shows the SENSE images and g-factor maps with increasing R for the 12 and 32-element surface coil arrays. SENSE images from the two coil arrays do not show apparent difference when R is 2. As R is increased to 3, noise amplification is locally observed for the 12-element array (Fig. 2a) while it is not apparent for the 32-element array (Fig. 2c). Increasing R to 5 amplifies noise over the entire image for the 12-element array (Fig. 2a). Noise is relatively much reduced at the image for the 32-element array at R = 5 (Fig. 2c). Coil g-factor maps for the 12-element coil array demonstrate that hotspots (high g-factor) increase rapidly at the image center with increasing R (Fig. 2b). However, the hotspots increase gradually with increasing R for the 32-element coil array (Fig. 2d). Additionally, the g-factor is much lower for the 32-element array (Fig. 2d) than for the 12-element array (Fig. 2b) at each reduction factor.

Figure 3 demonstrates a comparison between the mean g-factor (Fig. 3a), maximum g-factor (Fig. 3b), and AP (Fig. 3c) provided by 12 and 32-element coil arrays. The mean g-factor for the 32-element array rises relatively slowly with increasing R while the mean g-

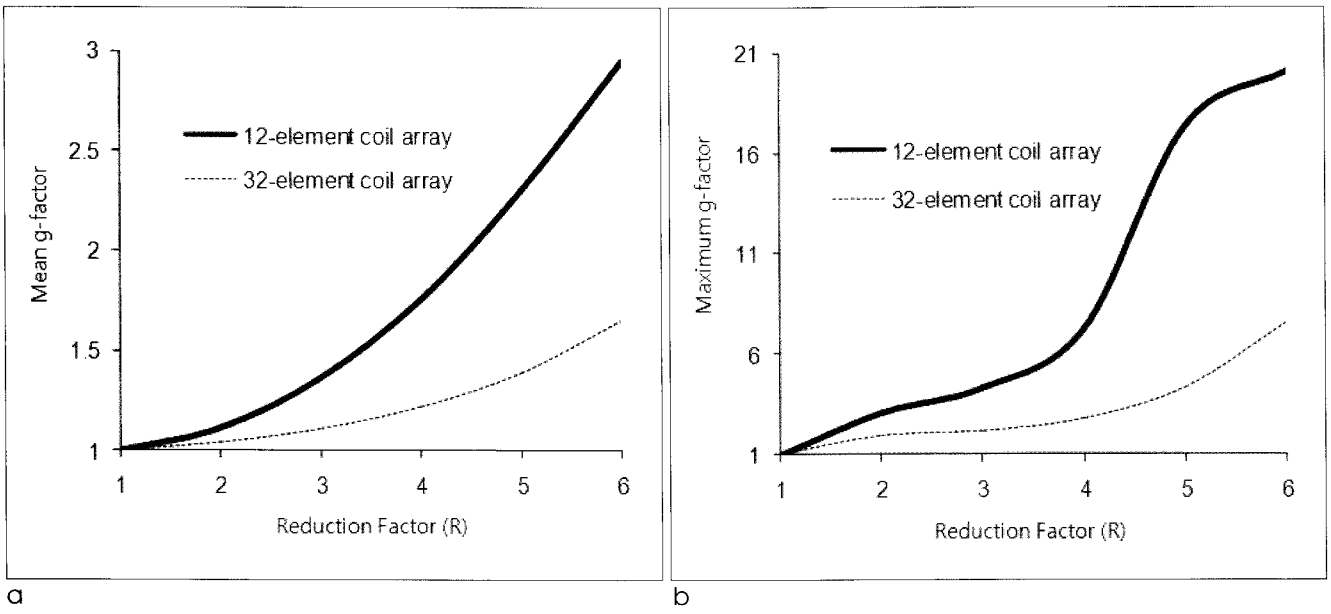

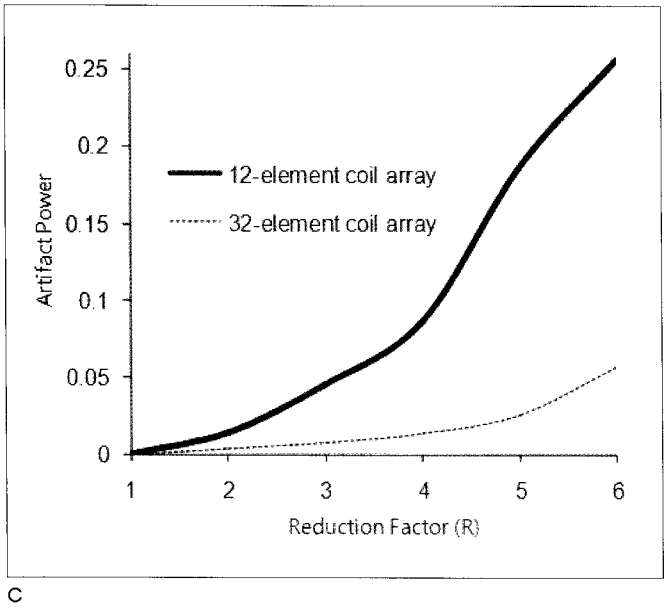

Fig. 3. Comparison of 12 and 32-element coil arrays using: (a) mean g-factor, (b) maximum g-factor, and (c) artifact power in SENSE reconstruction with the increase of reduction factor

factor for the 12-element array varies gradually at R $\leq$ 3 but rapidly at R > 3. This behavior of the curve in Figure 3a shows that noise amplification at R = 3 and 4 for the 32-element coil array corresponds to that at R = 2 and 3 for the 12-element coil array respectively. The mean g-factor in the 12-element coil array ranges between 1 and 2.95 while that in the 32-element coil array ranges between 1 and 1.65. The maximum g-factor for the 32-element coil array increases slowly at R $\leq$ 6 and ranges between 1 and 7.62. For the 12-element coil array, the maximum g-factor rises slowly at R $\leq$ 4 and increases rapidly at R > 4, ranging between 1 and 20.1. The AP curve shows tendencies similar to the maximum g-factor curve, ranging between 0 and 0.25 for the 12-element coil array and between 0 and 0.06 for the 32-element coil array.

Tables 1 and 2 show the mean g-factor, maximum g-factor, and AP for both the LAD and RCA orientations from the five volunteers. The g-factors and AP represent statistically significant difference between the two coil arrays for both the LAD and RCA orientations. 3 shows that the mean g-factor is sensitive to imaging orientations while the maximum g-factor and AP do not show statistical differences between the LAD and RCA orientations.

Representative LAD and RCA images reconstructed using SENSE (R = 4) and 3D maximum intensity projections (MIP) from 12 and 32-element coil array data sets are shown in Figure 4. The 32-element array images (Fig. 4b) demonstrate improved artifact and noise suppression compared to the 12-element array images (Fig. 4a).

Discussion

Parallel imaging with the 32-element surface coil array provides the acceleration beyond that achievable with a 12-element surface coil array for coronary artery orientations. It is feasible to significantly reduce artifact and noise even at high accelerations due to the improved g-factor of the 32-element coil array.

Noise originates predominantly from a subject rather than from the coil array and electronics. The induced noise is weighted by the spatial coil sensitivity profile. SNR can be enhanced by the reduction of the size of coil element. It is because the amplitude of noise detected in each coil is decreased while that of signal is preserved if all the coil images are combined. In parallel imaging, the achievable acceleration factor is limited to the number of coil elements located along the phase encoding direction, since better separation of the spatial sensitivity profiles enhances the suppression of aliasing artifact and noise. Compared with the 12-element coil array, the 32-element coil array provides higher SNR and lower g-factor because the size of each coil element is smaller and the spatial sensitivity profiles are more localized along the phase encoding direction.

For both the LAD and RCA orientations, the maximum g-factor with the 12-element coil array shows an abrupt increase with R > 4, representing that it is difficult to have more than four coil elements that

Table 2. Mean g-factor, Maximum g-factor, and Artifact Power in SENSE with Five Sets of RCA Data

		R = 2	R = 3	R = 4	R = 5	R = 6	Significance
Mean g-factor	12-element	1.08±0.029	1.32±0.046	1.82±0.12	2.64±0.19	3.63±0.32	P=1.98E-10
	32-element	1.03±0.0058	1.13±0.026	1.31±0.089	1.58±0.19	1.91±0.27	
Maximum g-factor	12-element	2.66±0.54	4.16±0.77	6.89±0.99	13.87±2.37	22.2±2.46	P=2.09E-10
	32-element	2.02±0.33	2.34±0.29	3.69±0.43	4.79±0.86	6.74±2.30	
Artifact Power	12-element	0.015±0.0018	0.038±0.0067	0.089±0.027	0.16±0.064	0.20±0.048	P=3.67E-05
	32-element	0.0089±0.0019	0.022±0.0013	0.039±0.0048	0.067±0.0059	0.099±0.022	

Table 3. Statistical Difference of Mean g-factor, Maximum g-factor, and Artifact Power for the Two Orientations: LAD and RCA

Mean g-factor		Maximum g-factor		Artifact Power	
12-element	32-element	12-element	32-element	12-element	32-element
P = 0.0069	P = 0.028	NS	NS	NS	NS

NS: Not Significant

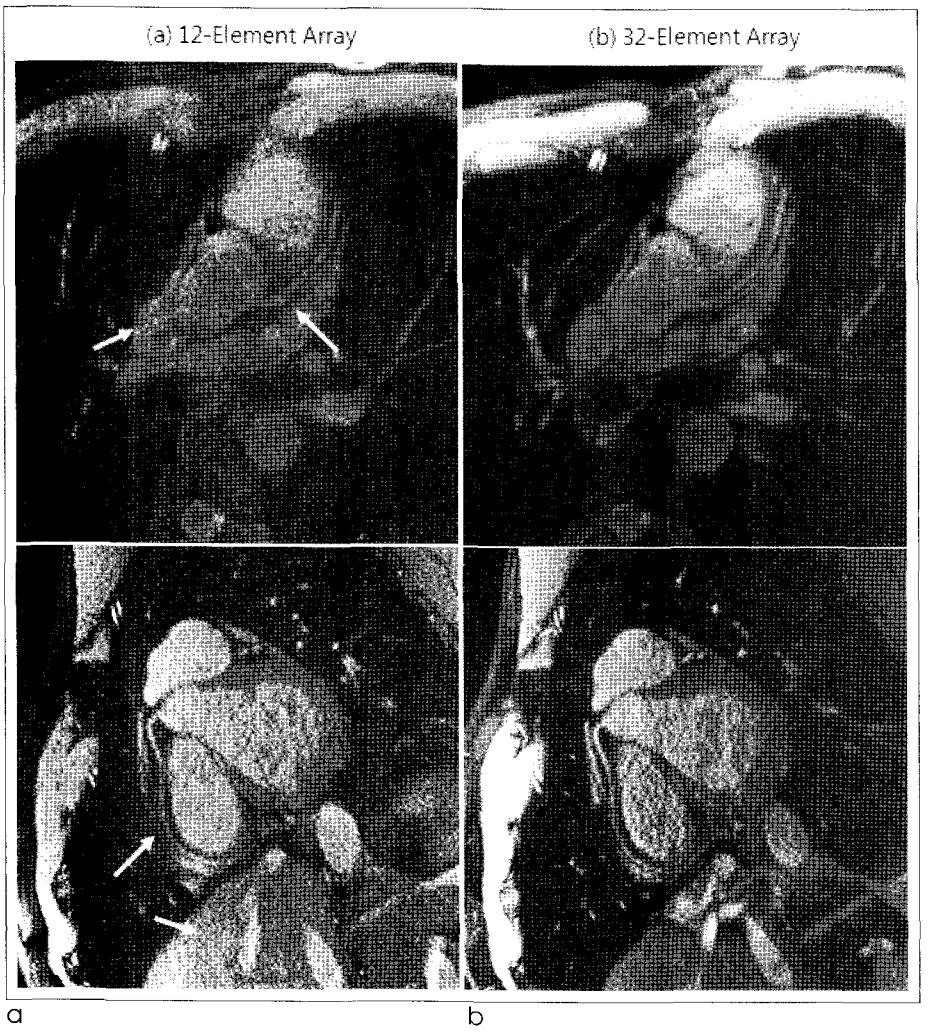

Fig. 4. Coronary artery images reconstructed using SENSE (R = 4) and 3D MIP with: (a) 12-element array and (b) 32-element array. Note increased SNR and improved vessel delineation in (b) over (a)

show the sufficient separation of spatial sensitivity profiles along the phase encoding direction. The reason the mean g-factor curve does not show the abrupt change with the increase of reduction factors is due to the averaging effect of the mean g-factor values over the ROI. The comparison of the maximum g-factors between the two coil arrays is highly dependent on the ROI, since the hotspots of the g-factor map varies spatially. To reduce the effect of the selection of ROI on the maximum g-factor, the ROI diameter was chosen large enough around the coronary arteries in the image.

The mean g-factor comparisons between the two coronary artery orientations shows that LAD is more favorable than RCA for parallel imaging with the current coil configurations. However, the two orientations presents nearly the same level of hotspots (maximum g-factor) in the g-factor map where the SENSE inversion is highly ill conditioned. It is because the number of coil elements is insufficient along the phase encoding direction as compared to the acceleration factor. If the g-factor rises, AP increases. The calculation of AP in the image domain is highly weighted in the high g-factor region, and has an averaging effect over the ROI. As a result, the AP curve in Figure 3c follows the mixed trend of both the maximum and mean g-factor curves.

Although the fully acquired data was decimated for the simulation of the parallel reconstruction in this work, it is expected that the motion-induced artifacts will be more reduced when the acceleration is applied in the clinical experiments, especially in the cardiac imaging, where the better spatial resolution can be achieved if the same imaging time is maintained.

In conclusion, parallel imaging with the 32-element surface coil array can provide acceptable SNR as well

as sufficient artifact and noise suppression for highly accelerated coronary MRA. The resulting acceleration may be exploited for either improving spatial resolution or enhancing 3D volume coverage.

Acknowledgement

This research was supported by the Basic Science Research Program through the National Research Foundation of Korea (NRF) funded by the Ministry of Education, Science and Technology (2009-0066543) and the Brain Korea 21 Project for Medical Science, Yonsei University.

References

1. Pruessmann KP, Weiger M, Scheidegger MB, Boesiger P. SENSE: sensitivity encoding for fast MRI. Magn Reson Med 1999;42(5):952-962
2. Sodickson DK, Manning WJ. Simultaneous acquisition of spatial harmonics (SMASH): fast imaging with radiofrequency coil arrays. Magn Reson Med 1997;38(4):591-603
3. Park J, McCarthy R, Li D. Feasibility and performance of breath-hold 3D true-FISP coronary MRA using self-calibrating parallel acquisition. Magn Reson Med 2004;52(1):7-13
4. Huber ME, Kozerke S, Pruessmann KP, Smink J, Boesiger P. Sensitivity-encoded coronary MRA at 3T. Magn Reson Med 2004;52(2):221-227
5. Weiger M, Pruessmann KP, Leussler C, Roschmann P, Boesiger P. Specific coil design for SENSE: a six-element cardiac array. Magn Reson Med 2001;45(3):495-504
6. Fattahi S, Rutt BK. Pushing The Speed Limit in SENSE using Novel Sampling Strategies. In: 2nd International Workshop on Parallel MRI, Zurich, 2005
7. Xu D, Jacob M, Liang ZP. Optimal Sampling of k-Space with Cartesian Grids for Parallel MR Imaging. In: Proceedings of the 11th Annual Meeting of ISMRM, Miami, 2005. p 2450
8. Lin FH, Kwong KK, Belliveau JW, Wald LL. Parallel imaging reconstruction using automatic regularization. Magn Reson Med 2004;51(3):559-567
9. Niendorf T, Hardy CJ, Cline H, et al. Highly Accelerated Single Breath-Hold Coronary MRA with Whole Heart Coverage using a Cardiac Optimized 32-element Coil Array. In: Proceedings of the 13th Annual Meething of ISMRM, Miami, 2005, p 702
10. Paul D, Hennig J. Comparison of different flip angle variation functions for improved signal behavior in SSFP sequences. In: Proceedings of the 12th Annual Meeting of ISMRM, Kyoto, 2004, p 2663

대한자기공명의과학회지 13:137-145(2009)

체적 지향형 호흡정지 자기공명 조영술의 가속화에 대한 32 채널 코일 어레이의 효용성

[1]연세대학교 의과대학 의과학과
[2]연세대학교 의과대학 영상의학과
[3]연세대학교 계산과학공학과

이현열[1,2] · 서진석[1,2] · 박재석[2,3]

목적: 각각 12개와 32개 요소 표면 코일 어레이를 사용한 가속율이 매우 큰 관상동맥 자기 공명 혈관조영술을 병렬 영상 기법에 적용하고 결과를 비교한다.

방법: 5명의 건강한 지원자에 대하여 1.5T 전신 자기공명영상장치에서 각각 12개와 32개 요소 표면 코일 어레이를 사용한 steady state free precession 자기공명 혈관조영술이 수행되었다. 각 지원자의 좌전하방관상동맥과 우관상동맥을 영상하여 데이터를 얻었다. 데이터는 병렬 영상을 위하여 1에서 6에 이르는 감소율로 부분 추출되었다. 양 코일 어레이 각각에 대하여 지형 인자의 평균, 극대, 그리고 인공물정도가 계산되었다.

결과: 모든 감소율에 있어서, 32개 요소 어레이가 12개 요소 어레이에 비하여 지형인자의 평균과 극대, 그리고 인공물 정도가 상당히 줄어들었다 ($P \ll 0.1$). 지형인자의 평균은 관상동맥의 영상 방향에 민감한 반면, 지형인자 극대치와 인공물정도는 영상 방향에 독립적이었다.

결론: 가속율이 매우 큰 관상동맥 자기공명 혈관조영술의 병렬 영상 적용에 있어 32개 요소 표면 코일 어레이를 사용함은 인공물과 잡음을 상당히 억제시킨다. 32개 요소 표면 코일 어레이를 사용하여 가속율을 증가시키는 것은 공간 해상도를 향상시키거나 3D 관상동맥 자기공명 혈관조영술에 있어서 체적 범위를 증가시킬 수 있는 가능성을 제공한다.

통신저자 : 박재석, (120-752) 서울시 서대문구 성산로 250, 연세대학교 의과대학 영상의학과
Tel. 82-2-2228-2397 Fax. 82-2-393-3035 E-mail: jaeseokpark@yonsei.ac.kr